

# LOAN DOCUMENT

PHOTOGRAPH THIS SHEET

①

DTIC ACCESSION NUMBER

LEVEL

INVENTORY

Tech. Paper 1293

DOCUMENT IDENTIFICATION

Aug 78

**DISTRIBUTION STATEMENT A**  
Approved for Public Release  
Distribution Unlimited

DISTRIBUTION STATEMENT

ACCESSION FOR

NTIS ☐ GRAM ☐  
DTIC ☐ TRAC ☐  
UNANNOUNCED ☐  
JUSTIFICATION ☐

BY

DISTRIBUTION/

AVAILABILITY CODES

DISTRIBUTION

AVAILABILITY AND/OR SPECIAL

A-1

DISTRIBUTION STAMP

DATE ACCESSIONED

DATE RETURNED

19990519 144

DATE RECEIVED IN DTIC

REGISTERED OR CERTIFIED NUMBER

PHOTOGRAPH THIS SHEET AND RETURN TO DTIC-FDAC

H  
A  
N  
D  
L  
E  
  
W  
I  
T  
H  
  
C  
A  
R  
E

# Friction and Wear of Metals With a Single-Crystal Abrasive Grit of Silicon Carbide - Effect of Shear Strength of Metal

Kazuhisa Miyoshi and Donald H. Buckley

AUGUST 1978

**NASA**

NASA Technical Paper 1293

Friction and Wear of Metals With  
a Single-Crystal Abrasive Grit  
of Silicon Carbide - Effect of  
Shear Strength of Metal

Kazuhisa Miyoshi  
*Kanazawa University*  
*Kanazawa, Japan*

Donald H. Buckley  
*Lewis Research Center*  
*Cleveland, Ohio*



National Aeronautics  
and Space Administration

**Scientific and Technical  
Information Office**

1978

# FRICION AND WEAR OF METALS WITH A SINGLE-CRYSTAL ABRASIVE GRIT OF SILICON CARBIDE - EFFECT OF SHEAR STRENGTH OF METAL

by Kazuhisa Miyoshi\* and Donald H. Buckley

Lewis Research Center

## SUMMARY

An investigation was conducted to examine the removal and plastic deformation of metal as a function of the metal properties when the metal is in sliding contact with a single-crystal abrasive grit of silicon carbide. Also examined was the friction force in sliding relative to the metal properties.

Four sets of sliding friction experiments were conducted. In the first two sets, spherical silicon carbide riders slid on flat metal surfaces: one set in dry argon, and the second set in oil. In the second two sets of experiments, spherical metal riders slid on flat silicon carbide surfaces: again one set in dry argon, and the second set in oil. Single-pass sliding experiments were conducted at 25° C with loads of 5 to 40 grams (0.049 to 0.39 N) at a sliding velocity of  $3 \times 10^{-3}$  m/min with a total sliding distance of 3 millimeters.

The results of the investigation indicate that the friction force in the plowing of the metal and the groove height (corresponding to the volume of the groove) are related to the shear strength of the bulk metal. That is, they decrease linearly as the shear strength of the bulk metal increases. Grooves are formed in metals primarily from plastic deformation, with occasional metal removal. The relation between the groove width  $D$  and the load  $W$  can be expressed by  $W = kD^n$ , which satisfies Meyer's law.

## INTRODUCTION

Abrasive wear is the mechanism involved in the finishing of many surfaces. Filing, sanding, lapping, and grinding of surfaces all involve abrasive wear.

---

\* Assistant Professor of Precision Engineering, Kanazawa University, Kanazawa, Japan; National Research Council - National Aeronautics and Space Administration Research Associate.

Khrushchov, and Babichev (ref. 1) found that the resistance of metals to abrasive wear was related to their relative static hardness under two-body conditions; that is, it was inversely proportional to the Vickers hardness  $H_V$  of the initial annealed metal to a Vickers hardness of 430 (tungsten). Avient, Goddard, and Wilman (ref. 2) theoretically and experimentally indicate that the resistance of metals to abrasive wear was inversely proportional to the Vickers hardness of the fully work-hardened surface region on abraded metal at a  $H_V$  of about 250. Similar results have been obtained by Rabinowicz, Dunn, and Russell (ref. 3) under three-body conditions. No attempt, however, has been made to explain in detail abrasive wear and friction in terms of the mechanical properties of metals such as shear strength. Further, there is a great lack of fundamental information relative to the friction energy dissipated in abrasive wear processes. Such information can lead to reducing the energy consumed in such operations as grinding.

The present investigation examined the removal and plastic deformation of metal in sliding contact with single-crystal abrasive grit of silicon carbide as a function of such metal properties as shear strength. Riders of 0.025- and 0.040-millimeter-radius spherical silicon carbide were used to simulate abrasive grit. The friction force in sliding was also examined relative to the metal properties.

Four sets of experiments were conducted. In the first two sets, spherical silicon carbide riders slid on flat metal surfaces: one set in dry argon, and the second set in oil. In the second two sets of experiments, spherical metal riders slid on flat silicon carbide surfaces: again one set in dry argon, and the second set in oil. The first two sets and the associated specimen configuration are such that friction and wear of the metals arise primarily from shearing at the interface or in the metal and from plowing in the metal. The second two sets and the associated specimen configuration are such that friction and wear of the metals arise primarily from shearing at the interface or in the metal. Single-pass sliding experiments were conducted at 25° C with loads of 5 to 40 grams (0.049 to 0.39 N) at a sliding velocity of  $3 \times 10^{-3}$  m/min with a total sliding distance of 3 millimeters.

## SYMBOLS

|       |  |
|-------|--|
| A     | projected area of contact, $\pi D^2/8$ |
| D     | width of a groove (wear track)         |
| H     | height of a groove (wear track)        |
| $H_V$ | Vickers hardness                       |
| k     | constant for material                  |

- k' constant for material
- m constant for material
- n constant for material (Meyer's index)
- P contact pressure during sliding, W/A
- r radius of spherical rider
- W normal load

## MATERIALS, APPARATUS, AND EXPERIMENTAL PROCEDURE

The single-crystal silicon carbide used in these experiments was a 99.9-percent-pure compound of silicon and carbon and had a hexagonal, close-packed crystal structure. The Knoop hardness was 2954 in the  $\langle 10\bar{1}0 \rangle$  direction and 2917 in the  $\langle 11\bar{2}0 \rangle$  direction on the basal plane of silicon carbide (ref. 4). The titanium was 99.97 percent pure, and the copper was 99.999 percent pure. All the other metals were 99.99 percent pure, as shown in table I.

The apparatus used in this investigation is shown schematically in figure 1. The apparatus is described in reference 5.

### Specimen Preparation

The surfaces of the single-crystal silicon carbide and metal pin specimens (riders) were hemispherical and were polished with approximately 3-micrometer-diameter diamond powder and then 1-micrometer-diameter aluminum oxide ( $\text{Al}_2\text{O}_3$ ) powder. The radii of curvature of the silicon carbide spherical riders were 0.04 and 0.025 millimeter, as shown in figure 2. The orientations of the single-crystal silicon carbide riders are also shown in figure 2. The radius of curvature of all the metal riders was 0.79 millimeter (1/32 in.). The surfaces of both the silicon carbide and metal disk specimens were also polished with 3-micrometer-diameter diamond powder and then 1-micrometer-diameter aluminum oxide powder.

### Test Procedure

Both the silicon carbide and metal surfaces were rinsed with 200-proof ethyl alcohol before use. The friction experiments were single pass over a total sliding distance of 3 millimeters at a sliding velocity of 3 millimeters per minute. They were conducted in

dry argon ( $\text{H}_2\text{O} < 20$  ppm) at atmospheric pressure and in degassed mineral oil. Typical properties of the mineral oil appear in table II. All the experiments were conducted at  $25^\circ\text{C}$ .

The widths of the grooves (wear tracks) reported herein were obtained by averaging measurements of 10 surface-profile records.

## RESULTS AND DISCUSSION

### Friction and Wear of Metal Surfaces in Contact with Silicon Carbide

#### Rider in Argon at Atmospheric Pressure

Sliding friction experiments were conducted with 0.04-millimeter-radius spherical silicon carbide riders in contact with disk surfaces of various metals in argon at atmospheric pressure. The sliding involves plastic flow and the generation of metal wear debris, typical examples of which are shown in figures 3 to 5. Figure 3 shows a typical scanning electron micrograph and surface profile of a wear track (groove) made on an iron surface by the sliding of a silicon carbide rider. (Surface profiles were recorded by a surface profilometer.) Figure 3 reveals that the sliding action resulted in a permanent groove in the metal surface, with considerable deformed metal piled up along the sides of the groove. More detailed examination of this groove revealed further evidence of metal wear debris, as shown in figure 4. The wear debris particles are generated primarily on the sides of the wear track. Moreover, examination of the surface of the silicon carbide rider revealed transferred metal wear particles, as shown in figure 5. Figure 5(a) presents a scanning electron micrograph of the surface of the silicon carbide rider at its tip after it had slid on an iron surface. The X-ray energy dispersive analysis for iron on the silicon carbide surface is presented in figure 5(b); the concentrations of white spots correspond to the wear particles of iron transferred.

Thus, the foregoing typical results reveal that both plastic deformation of metal and the generation of metal wear debris occur as a result of sliding friction between a spherical silicon carbide rider and a metal surface. The amount of metal removed, however, was very much less than the volume of the groove (wear track) plowed out by the silicon carbide rider. Avient, et al. (ref. 2) indicate that abrasion on dry emery leads to an amount of wear (metal removal) corresponding to only about 10 percent of the volume of the grooves plowed out by the abrasives.

Figure 6 is a schematic representation of the lateral and longitudinal cross-sectional views of a groove. The width  $D$  and height  $H$  of a groove (wear track width and height) are defined in figure 6. Contact pressure  $P$  during sliding may, then, be defined by  $P = W/A$ , where  $W$  is the applied normal load and  $A$  is the projected area

of contact and is given by  $A = \pi D^2/8$  (only the front half of the rider is in contact with the flat specimen).

The groove widths  $D$  generated by a 0.04-millimeter-radius silicon carbide rider are presented for a number of metals in figure 7 as a function of the applied load. The relation between  $D$  and the load  $W$  can be expressed by  $W = kD^n$ , which is known as Meyer's law (ref. 6). The value of  $n$  as determined herein for cubic and hexagonal metals lies between 2.0 and 2.2, except for titanium and zirconium. With titanium and zirconium,  $n$  is near 2.8. The  $n$ -value of titanium and zirconium may differ from those of other hexagonal metals because titanium and zirconium do not slip predominantly on the basal planes (slip plane, (0001); slip direction,  $\langle 11\bar{2}0 \rangle$ ) such as do the metals magnesium, cobalt, and rhenium. Titanium and zirconium slip predominantly on the prismatic planes (slip plane;  $(10\bar{1}0)$ , slip direction;  $\langle 11\bar{2}0 \rangle$ ) during plastic deformation.

With a spherical silicon carbide rider (radius, 0.04 mm), the metal groove is formed primarily from plastic deformation of the metal, and metal removal occurs occasionally along the sides of the groove.

The groove height  $H$  (peak-to-valley height of the groove) was also measured from the profile records, as already shown in figure 3. The groove heights generated with the 0.04-millimeter-radius silicon carbide rider are presented for a number of metals in figure 8 as a function of the applied load. The relation between  $H$  and the load  $W$  can be expressed by  $W = k'H^m$ , where  $k'$  and  $m$  are constants for the metal under examination. The value of  $m$  for cubic and hexagonal metals lies between 1.1 and 1.2.

Figure 9 presents the coefficients of friction and the groove heights for various metals after sliding experiments at a load of 20 grams in argon at atmospheric pressure. There is no obvious correlation between coefficient of friction and contact pressure ( $P = W/A$ ), which depends on the metal properties. The relationship between groove height and contact pressure is a nearly linearly decreasing one, but the rate of decrease (slope) changes at a contact pressure of about 300 kg/mm<sup>2</sup>. These results are comparable to those obtained by Avient, Goddard, and Wilman (ref. 2) for various metals initially wet abraded on no. 3 emery paper and then slid under a 300-gram load on dry grade-3 emery paper (particles of 150- $\mu$ m mean diameter). Avient, et al., established that, for Vickers hardness  $H_V$  of the abraded metal to about 250, the inverse of the abrasive wear rate is approximately proportional to  $H_V$  but that the mean locus appears to curve upward away from the  $H_V$  axis at higher  $H_V$ . Thus, the results of figure 9 are similar to those obtained by Avient, et al. (ref. 2) in the full-scale wear test.

The stress in the metal, if the stress is applied to only a very small area of the contacting surface, is evidently complicated. Therefore, the shear and flow properties of the metal in abrasive wear processes have been indirectly expressed by means of static Vickers hardness (refs. 1 and 2); scratch hardness (ref. 7); mean stress supporting load (ref. 8); contact pressure (fig. 9); plowing stress (ref. 7); mean stress opposing sliding (ref. 8); and so on.



On the other hand, the anisotropies of deformation and friction of single crystals in the abrasive wear processes have been explained in terms of the distribution of resolved shear stresses acting on the slip systems in crystals during sliding (ref. 9). The concept of shear stress, however, has been only slightly related to the abrasive friction-and-wear properties of polycrystalline metals because the mechanism of deformation is quite complicated.

The ultimate shear strength of metals is very strongly dependent on the mean contact pressure, as shown in figure 10 (ref. 10). Figure 10 presents the ultimate shear strengths of various metals measured at mean hydrostatic pressures of 100 to 500 kg/mm<sup>2</sup>. The ultimate shear strength of a metal is increased with increasing applied hydrostatic pressure.

Figure 11 presents the coefficients of friction and the groove heights for various metals as a function of shear strength. The shear strength was estimated from the contact-pressure data in figure 9 by using the relation between hydrostatic pressure and shear strength shown in figure 10. The relation between the groove height and the shear strength of the metal shows that  $H$  decreases linearly with shear strength, except for molybdenum and tungsten, which have the greatest shear strengths.

A correlation between coefficient of friction and shear strength is not clear from figure 11. The coefficient of friction in figure 11 may be governed by two factors: (1) shearing at the interface and (2) plowing in the metal. The shearing force at the interface in dry friction is comparable in magnitude to the plowing force in the metal and depends on the nature of the interface. It is, therefore, anticipated that there is no obvious relationship between coefficient of friction and shear strength in figure 11 because the coefficient of friction is strongly influenced by variations of shearing force at the interface. This subject is discussed more fully in succeeding sections.

#### Friction of Metal Riders Sliding on Silicon Carbide Disks

Sliding friction experiments were conducted with spherical metal riders in contact with disks of silicon carbide (0001) surface in both argon at atmospheric pressure and in mineral oil. The friction data for various metals are presented in figure 12.

In argon at atmospheric pressure, the metal rider slides on the silicon carbide disk and shearing at the interface is primarily responsible for the friction behavior observed. The coefficients of friction in argon at atmospheric pressure are all less than 0.2. The metals exhibit a variation in friction, as anticipated in the preceding section.

The results of figure 11, in which the silicon carbide rider plowed a groove in the metal surface, reveal that shearing at the interface and plowing of the bulk metal are responsible for the friction behavior observed. The shearing force is approximately the same as the plowing force; this is arrived at by comparing the results in figures 11

and 12, except those for magnesium, aluminum, and zirconium. Although the shearing force at the interface and the plowing force are usually separable, with magnesium, aluminum, and zirconium, shearing at the interface and plowing of the metal seem to interact and are not separable in figure 11.

On the other hand, the coefficients of friction in oil are all approximately 0.05. The variation in friction for various metals is negligibly small. It is, therefore, anticipated that sliding experiments in oil, in which a hard silicon carbide rider plows a groove in a metal surface, may reveal a relationship between the coefficient of friction and a property of the bulk metal such as shear strength.

### Friction and Wear of Metal Surfaces in Contact with Silicon Carbide Rider in Oil

Sliding friction experiments were conducted with 0.04-millimeter-radius spherical silicon carbide riders in contact with surfaces of various metal disks in mineral oil. Figure 13 presents the coefficient of friction and the groove height for various metals at a load of 20 grams. In figures 13(a) and (b) the coefficient of friction and the groove height correlate with the shear strength of the metal, except for molybdenum and tungsten, as might be anticipated from figure 9. The relationship between the coefficient of friction and the shear strength is a linearly decreasing one as is the relationship between groove height and shear strength. Figure 13(c) presents the relationship between the contact pressure during sliding and the shear strength estimated from the contact-pressure data by using the relation of figure 10. The contact pressure is approximately proportional to the shear strength.

In the results in figure 13, however, molybdenum and tungsten were exceptions. With these metals the grooves produced by plowing of the rider were the smallest for all the metals. There may be a lower limit to the validity of the correlation between the coefficient of friction or the groove height and the shear strength. This lower limit seems to depend (1) on the geometry of the rider, that is, the radius of the spherical rider, and (2) on the load. A ratio of groove width to rider radius of about 0.25 may be the lower limit of the validity in figure 13.

Sliding friction experiments were also conducted with a spherical silicon carbide rider having a smaller radius (0.025 mm) in contact with a metal disk in mineral oil. The coefficients of friction, the groove heights, and the contact pressures are presented as a function of shear strength in figure 14. Because large grooves were produced in magnesium, aluminum, copper, zirconium, and iron, experiments with these metals were conducted at a load of 5 grams. Because relatively smaller grooves were produced in titanium, nickel, rhodium, molybdenum, and tungsten, experiments with these metals were conducted at a load of 20 grams.

In figure 14, the coefficient of friction and the groove height correlate with the shear strength of the metal, and the relationships are approximately linearly decreasing ones without exception. In this experiment, the ratio of the groove width to the rider radius  $D/r$  ranged from about 0.36 to 0.5. Thus, the coefficient of friction, particularly the plowing term in that coefficient, and the groove height corresponding to the groove volume may be governed by two factors: (1) the shear strength at the interface and (2) the shear strength of the bulk metal. In figure 14, the contact pressure is nearly proportional to the shear strength of the metal.

### CONCLUSIONS

As a result of sliding friction experiments conducted with spherical single-crystal silicon carbide riders in sliding contact with various metals and with metal riders sliding against silicon carbide flats - to allowing for the separation of shearing and plowing effects in sliding - the following conclusions were drawn:

1. Both the friction force in the plowing of the metal and the groove height corresponding to the groove volume are related to the shear strength of the metal; that is, they decrease linearly with the ultimate shear strength of the bulk metal.
2. Grooves are formed in metals primarily from plastic deformation, with occasional metal removal.
3. The relationship between the groove width  $D$  and the applied load  $W$  can be expressed by  $W = kD^n$ , which satisfies Meyer's law. The value of  $n$  for cubic and hexagonal metals lies between 2.0 and 2.2, except for titanium and zirconium. For titanium and zirconium,  $n$  is near 2.8.

Lewis Research Center,  
National Aeronautics and Space Administration,  
Cleveland, Ohio, April 27, 1978,  
506-16.

### REFERENCES

1. Khrushchov, M. M.; and Babichev, M. A.: Resistance to Abrasive Wear and Elasticity Modulus of Metals and Alloys. Sov. Phys. -Dokl., vol. 5, 1960-1961, pp. 410-412.
2. Avient, B. W. E.; Goddard, J.; and Wilman, H.: An Experimental Study of Friction and Wear During Abrasion of Metals. Proc. Roy. Soc. (London), Series A, vol. 258, no. 1293, 18 Oct. 1960, pp. 159-180.

3. Rabinowicz, E.; Dunn, L. A.; and Russell, P. G.: A Study of Abrasive Wear Under Three-Body Conditions. *Wear*, vol. 4, 1961, pp. 345-355.
4. Shaffer, Peter T. B.: Effect of Crystal Orientation on Hardness of Silicon Carbide. *J. Am. Ceram. Soc.*, vol. 47, no. 9, Sept. 1964, p. 466.
5. Miyoshi, Kazuhisa; and Buckley, Donald H.: Friction and Deformation Behavior of Single-Crystal Silicon Carbide. NASA TP-1053, 1977.
6. Tabor, David: *Hardness of Metals*. Oxford Univ. Press (London), 1950, pp. 6-18.
7. Gane, N.; and Skinner, J.: The Friction and Scratch Deformation of Metals on a Micro Scale. *Wear*, vol. 24, 1973, pp. 207-217.
8. Childs, T. H. C.: The Sliding of Rigid Cones Over Metals in High Adhesion Conditions. *Int. J. Mech. Sci.*, vol. 12, 1970, pp. 393-403.
9. Bowden, F. P.; and Brookes, C. A.: Frictional Anisotropy in Nonmetallic Crystals. *Proc. Roy. Soc. (London), Series A*, vol. 295, no. 1442, Dec. 6, 1966, pp. 244-258.
10. Bridgman, P. W.: *Shearing Phenomena at High Pressures, Particularly in Inorganic Compounds*. *Proc. Am. Acad. Arts Sci.*, vol. 71, 1937, pp. 387-460.
11. Barrett, C. S.: *Structure of Metals, Crystallographic Methods, Principles, and Data*. McGraw-Hill Book Co., Inc., 1943, pp. 552-554.
12. Gschneidner, Karl A., Jr.: Physical Properties and Interrelationships of Metallic and Semimetallic Elements. *Solid State Physics*, vol. 16, F. Seitz and D. Turnbull, eds., Academic Press, 1965, pp. 275-426.

TABLE I. - CRYSTALLINE, PHYSICAL, AND CHEMICAL PROPERTIES OF METALS

| Metal      | Purity,<br>percent<br>(a) | Crystal structure<br>at 25° C<br>(b) | Lattice<br>constant,<br>Å<br>(10 <sup>-10</sup> m)<br>(b) | Cohesive energy     |                | Shear modulus         |                              |
|------------|---------------------------|--------------------------------------|---|---------------------|----------------|-----------------------|------------------------------|
|            |                           |                                      |   | J/(g)(atom)         | kcal/(g)(atom) | Pa                    | kg/cm <sup>2</sup>           |
| Iron       | 99.99                     | Body-centered cubic                  | a = 2.8610  | 416×10 <sup>3</sup> | 99.4           | 8.15×10 <sup>10</sup> | 0.831±0.006×10 <sup>-6</sup> |
| Chromium   |                           | ↓                                    | a = 2.8786  | 395                 | 94.5           | 11.7                  | 1.19                         |
| Molybdenum |                           |                                      | a = 3.1403  | 657.3               | 157.1          | 11.6                  | 1.18                         |
| Tungsten   |                           |                                      | a = 3.1586  | 835.5               | 199.7          | 15.3                  | 1.56±0.04                    |
| Aluminum   |                           | Face-centered cubic                  | a = 4.0414  | 322                 | 76.9           | 2.66                  | 0.271±0.001                  |
| Copper     | 99.999                    | ↓                                    | a = 3.6080  | 338                 | 80.8           | 4.51                  | 0.460±0.015                  |
| Nickel     | 99.99                     |                                      | a = 3.5169  | 428.0               | 102.3          | 7.50                  | 0.765                        |
| Rhodium    |                           | ↓                                    | a = 3.7956  | 556.5               | 133.0          | 14.7                  | 1.50±0.03                    |
| Magnesium  |                           | Hexagonal close-packed               | a = 3.2022<br>c = 5.1991                                  | 148                 | 35.3           | 1.74                  | 0.177                        |
| Zirconium  |                           |                                      | a = 3.223<br>c = 5.123                                    | 609.6               | 145.7          | 3.41                  | 0.348±0.008                  |
| Cobalt     |                           |                                      | a = 2.507<br>c = 4.072                                    | 425.5               | 101.7          | 7.64                  | 0.779                        |
| Titanium   | 99.97                     |                                      | a = 2.953<br>c = 4.729                                    | 469.4               | 112.2          | 3.93                  | 0.401±0.005                  |
| Rhenium    | 99.99                     | ↓                                    | a = 2.7553<br>c = 4.4493                                  | 779.1               | 186.2          | 17.9                  | 1.82                         |

<sup>a</sup>Manufacturer's analysis.<sup>b</sup>From ref. 11.<sup>c</sup>From ref. 12.TABLE II. - MINERAL OIL PROPERTIES<sup>a</sup>

|                                      |                              |
|--------------------------------------|------------------------------|
| Chemical type . . . . .              | Naphthenic mineral oil       |
| Viscosity, m <sup>2</sup> /sec (cS): |                              |
| At 38° C . . . . .                   | 73.4×10 <sup>-6</sup> (73.4) |
| At 99° C . . . . .                   | 8.35×10 <sup>-6</sup> (8.35) |
| Specific gravity:                    |                              |
| At 16° C . . . . .                   | 0.880                        |
| At 25° C . . . . .                   | 0.875                        |
| Pour point, °C . . . . .             | -18                          |
| Flashpoint, °C . . . . .             | 224                          |

<sup>a</sup>Manufacturer's analysis.

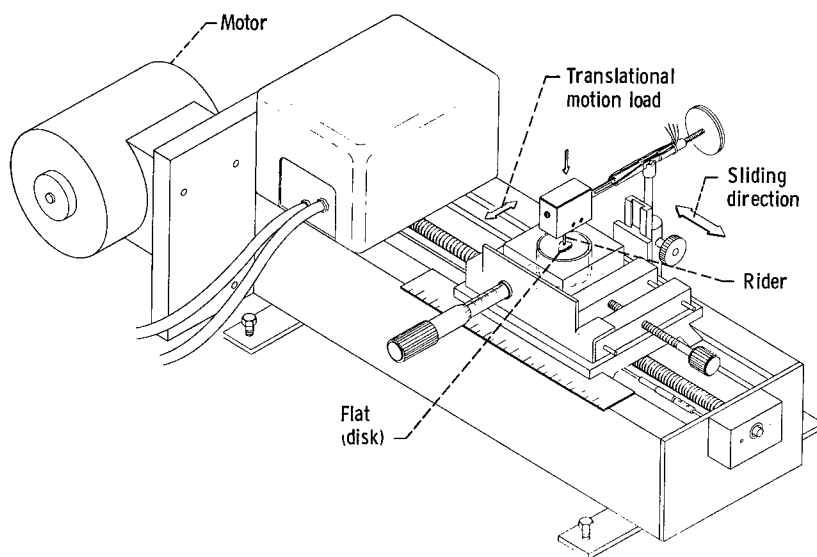
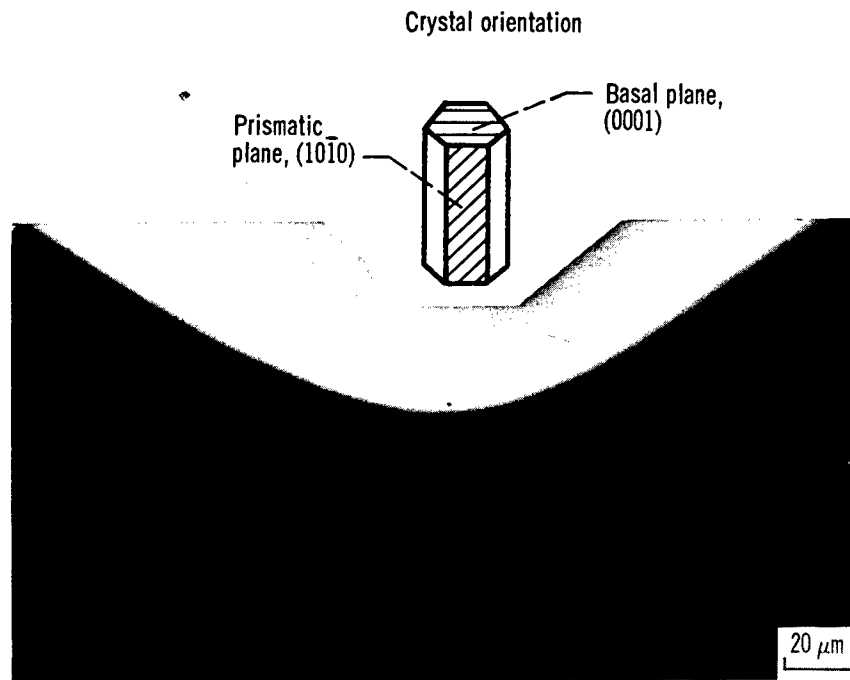
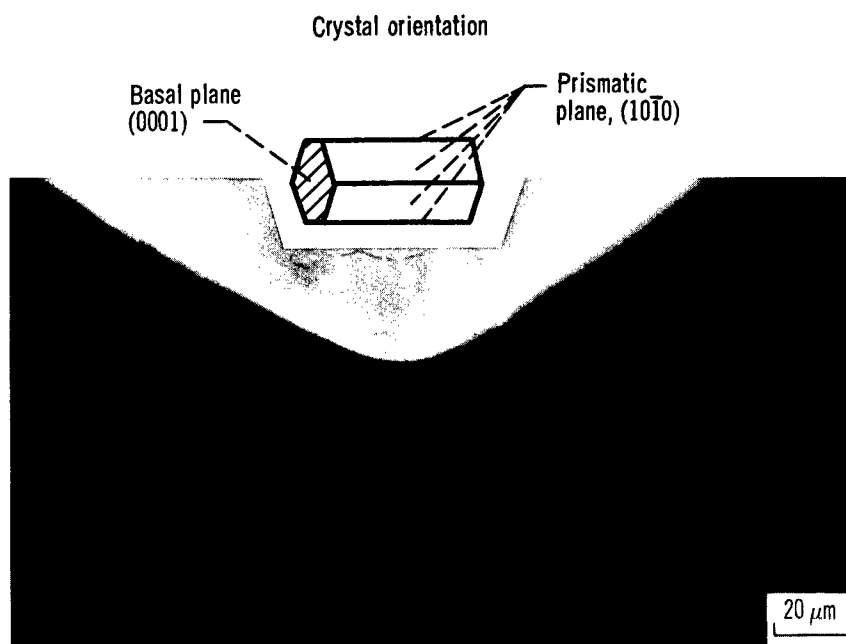


Figure 1. - Friction and wear apparatus.

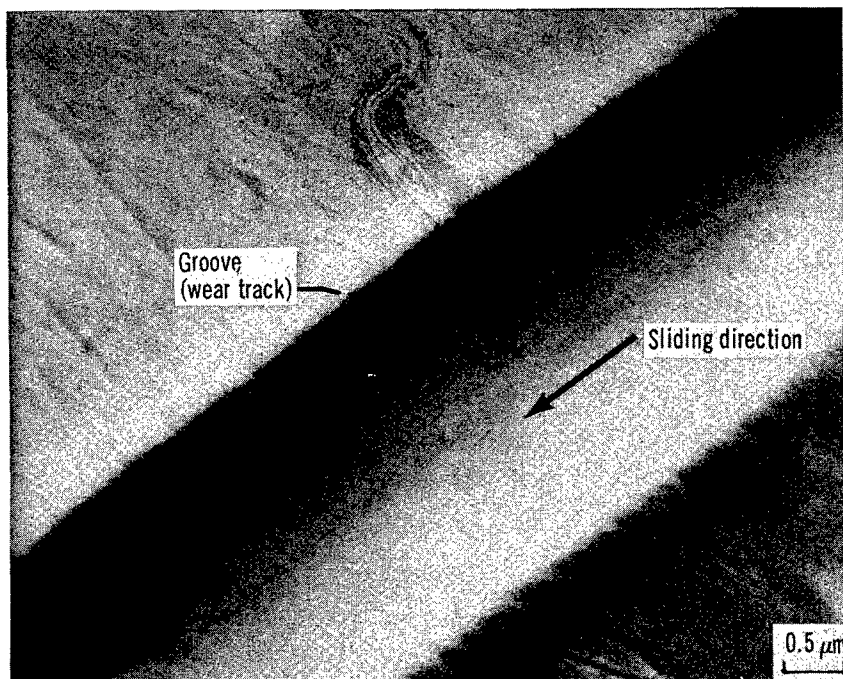


(a) 0.04-Millimeter-radius rider.

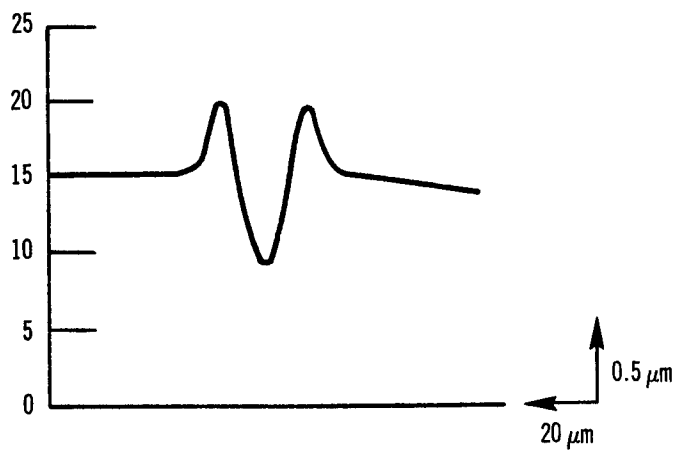


(b) 0.025-Millimeter-radius rider.

Figure 2. - Spherical silicon carbide riders.



(a) Scanning electron micrograph.



(b) Surface profile. Load, 30 grams.

Figure 3. - Groove on iron surface. Single-pass sliding of 0.04-millimeter-radius silicon carbide rider; sliding velocity, 3 mm/min; load, 30 grams (0.29 N); temperature, 25° C; environment, argon; pressure, atmospheric.



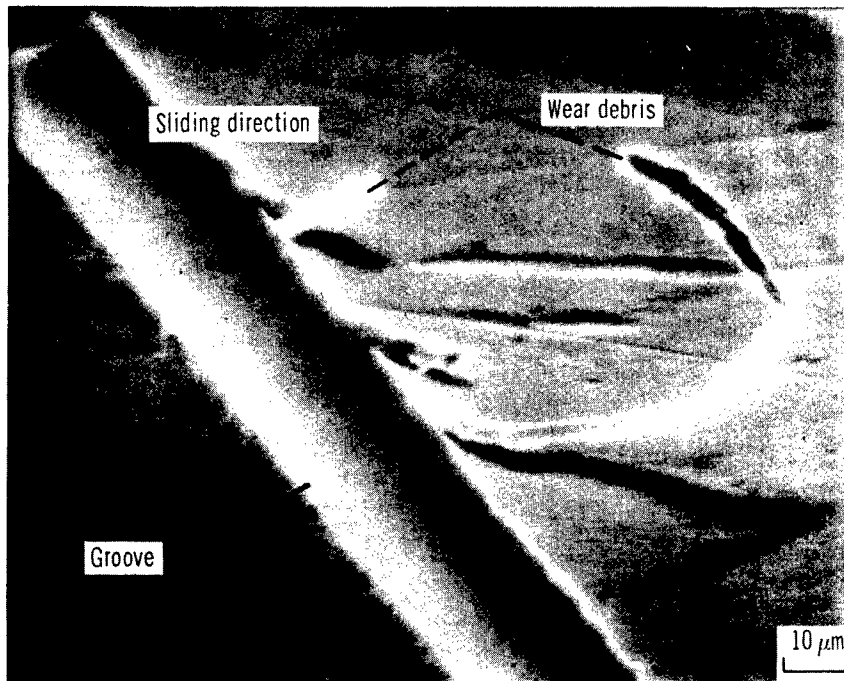
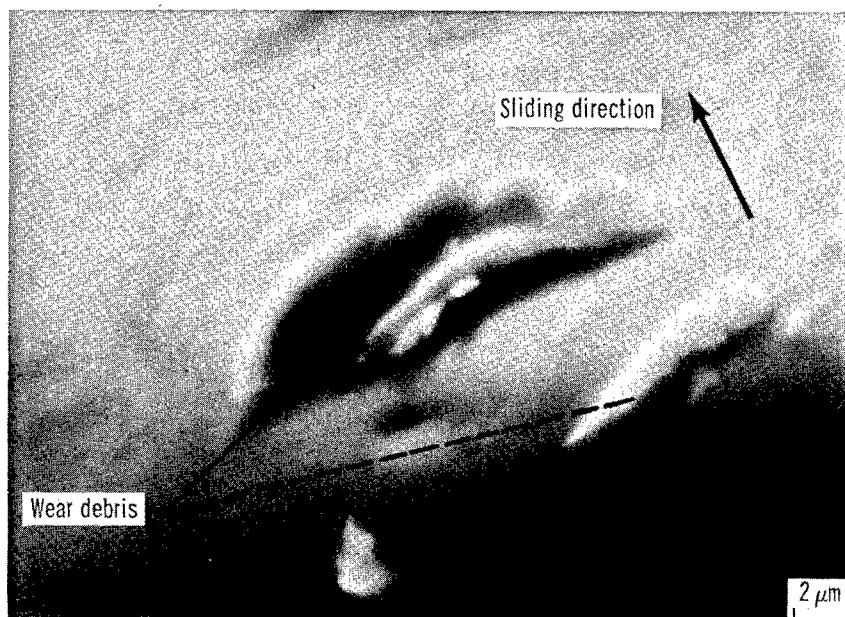
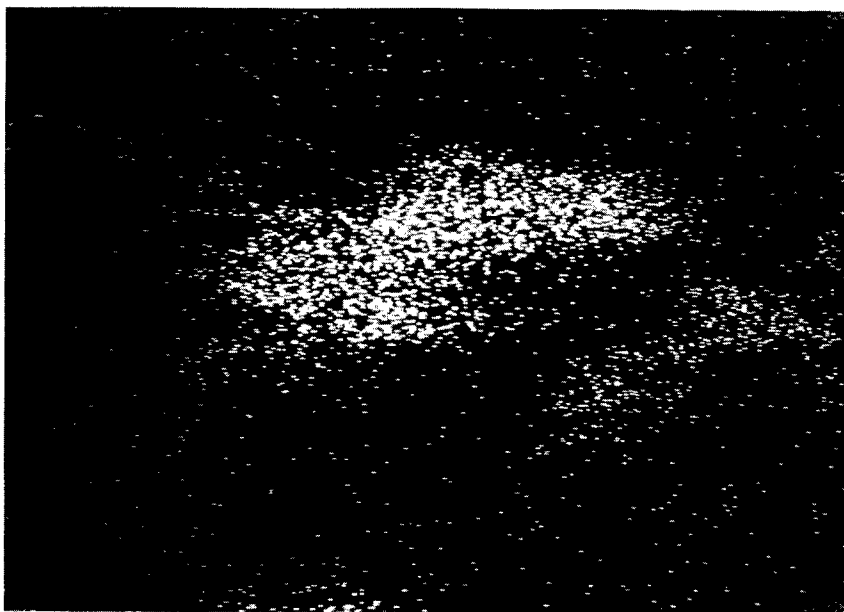


Figure 4. - Iron wear debris and grooves on iron surface. Single-pass sliding of 0.04-millimeter-radius silicon carbide rider; sliding velocity, 3 mm/min; load, 25 grams (0.25 N); temperature, 25° C; environment, argon; pressure, atmospheric.



(a) Iron wear debris transferred to silicon carbide.



(b) Iron  $K_{\alpha}$  X-ray map of silicon carbide;  $5.5 \times 10^3$  counts.

Figure 5. - Iron wear debris transferred to silicon carbide surface as a result of single pass of 0.04-millimeter-radius silicon carbide rider. Sliding velocity, 3 mm/min; load, 25 grams (0.25 N); temperature, 25° C; environment, argon; pressure, atmospheric.

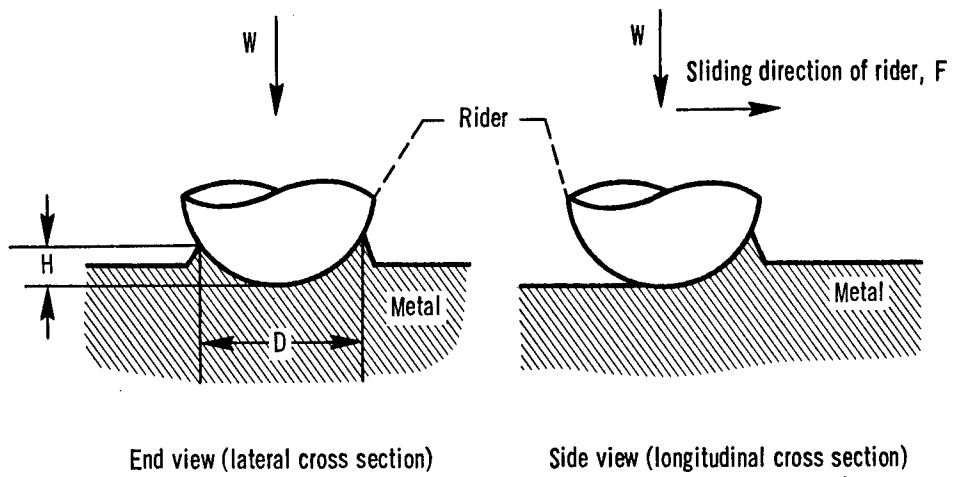


Figure 6. - Deformation of metal.

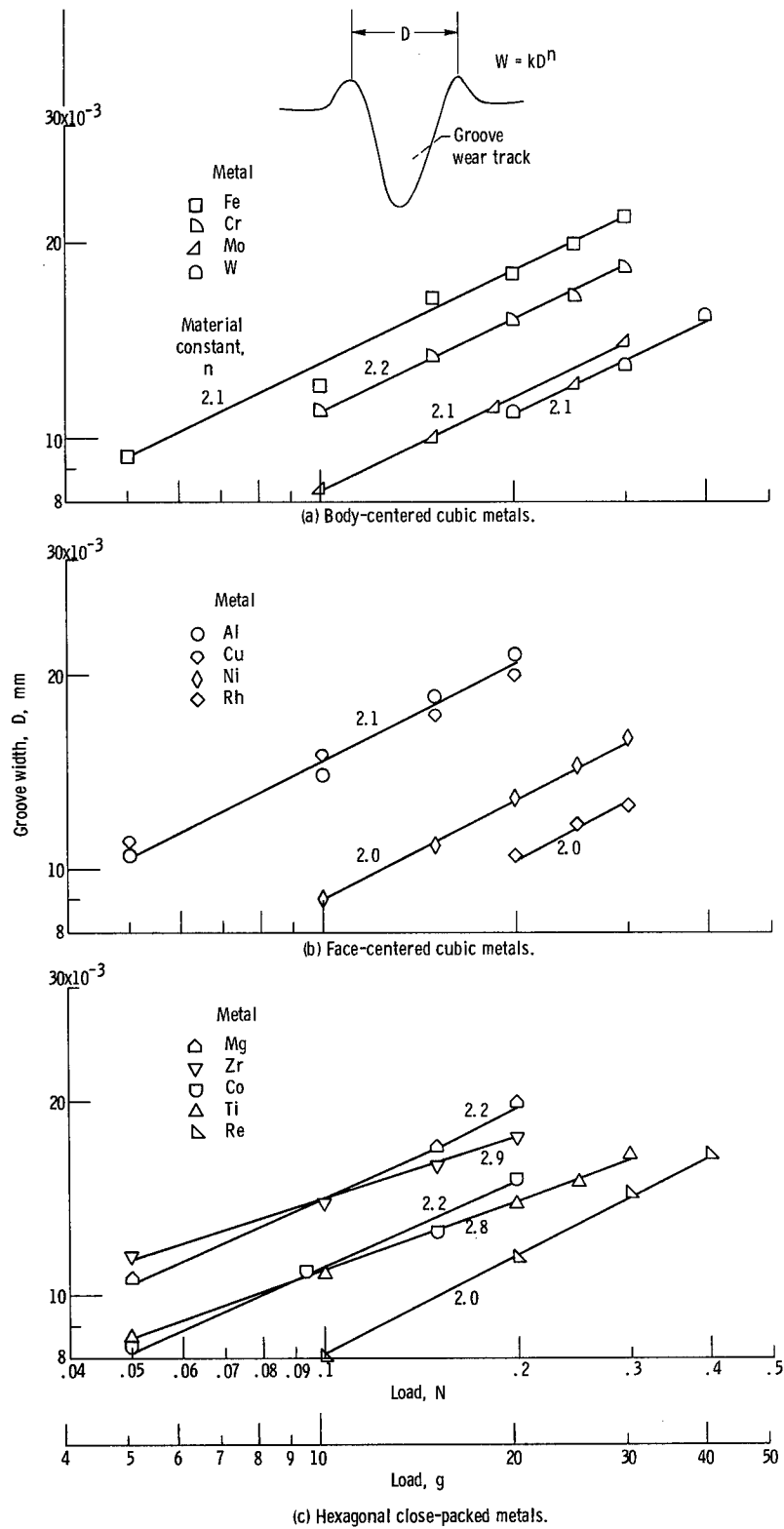


Figure 7. - Groove width as a function of load for various metals. Single-pass sliding of 0.04-millimeter-radius silicon carbide rider; sliding velocity, 3 mm/min; temperature, 25°C; environment, argon; pressure, atmospheric.

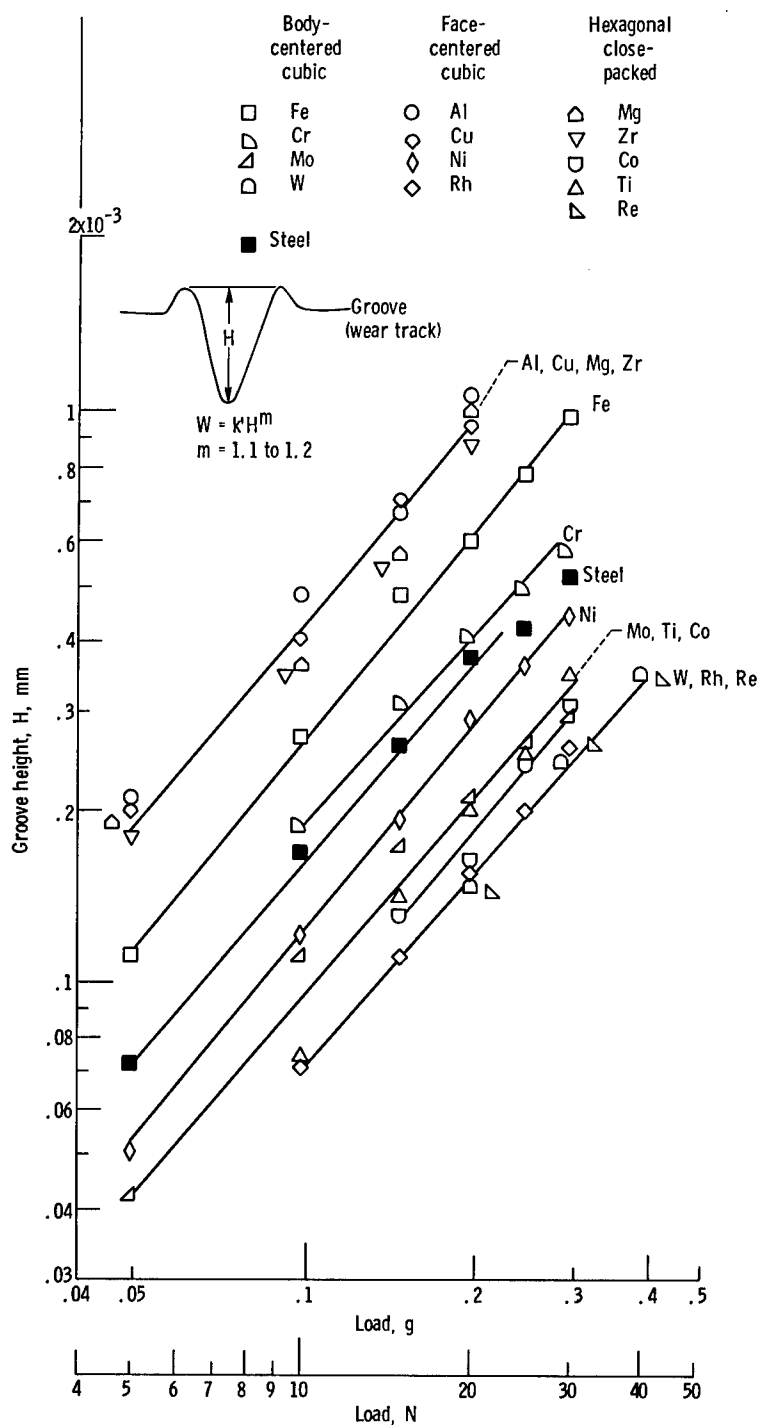


Figure 8. - Groove height (peak-to-valley height) as a function of load for various metals. Single-pass sliding of 0.04-millimeter-radius silicon carbide rider; sliding velocity, 3 mm/min; temperature, 25°C; environment, argon; pressure, atmospheric.

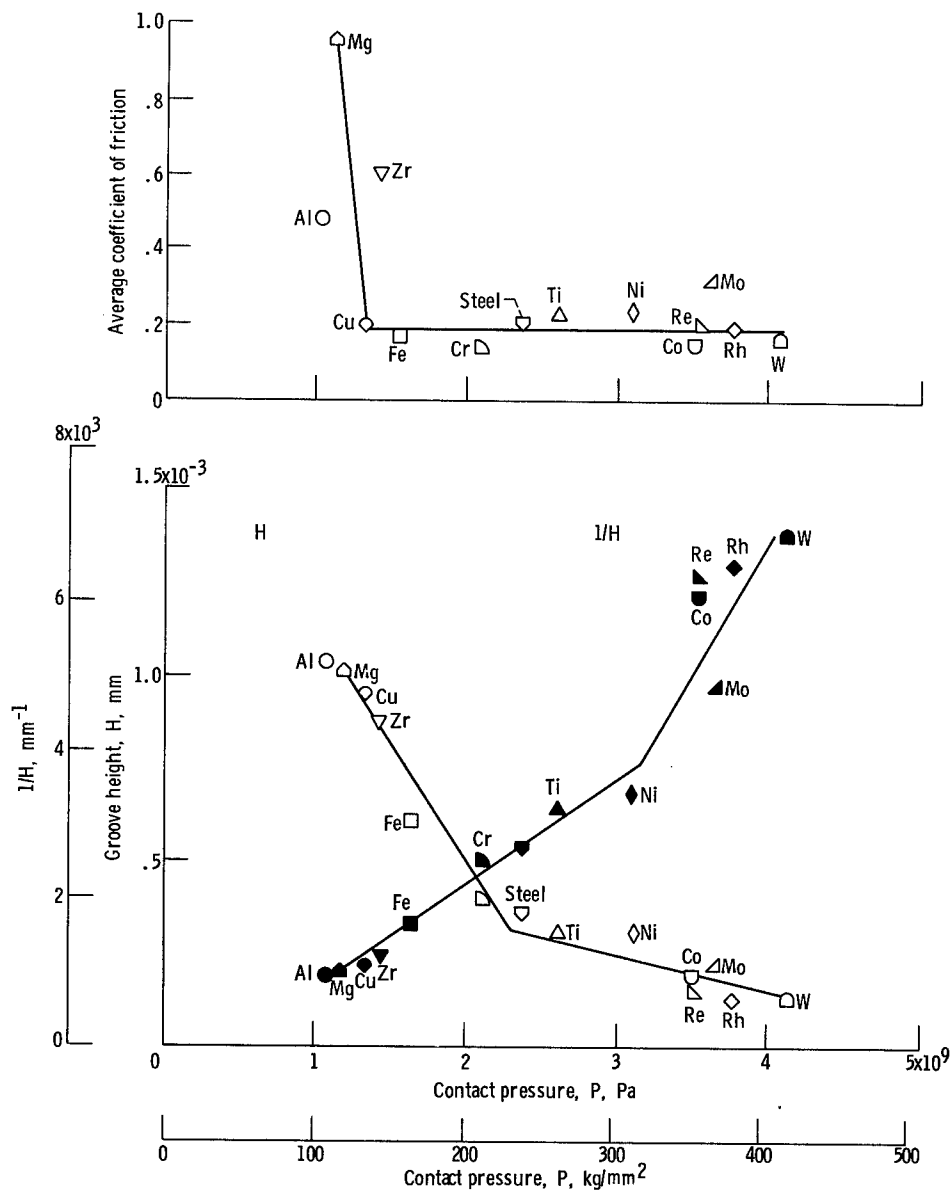
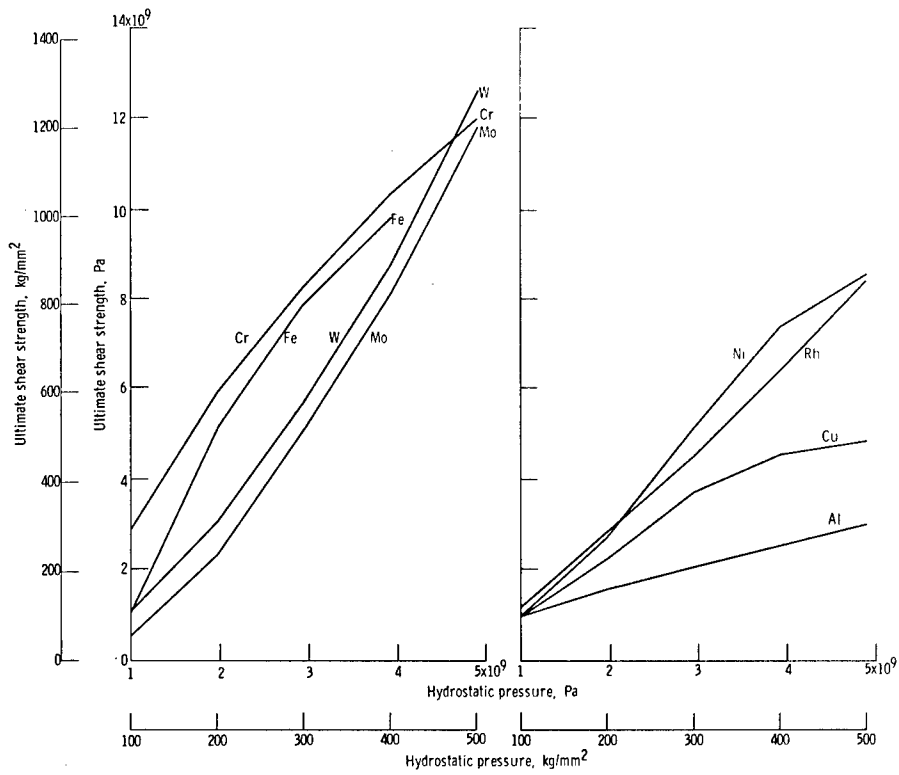
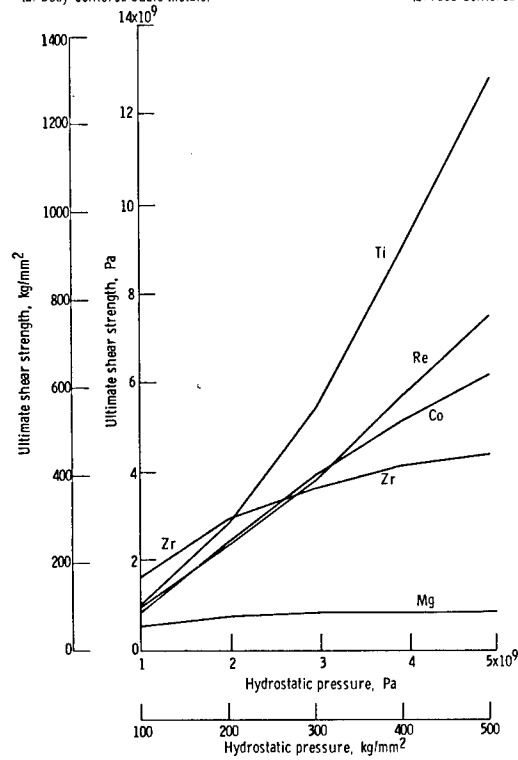


Figure 9. - Coefficient of friction and groove height as a function of contact pressure for various metals. Single-pass sliding of 0.04-millimeter-radius silicon carbide rider; sliding velocity, 3 mm/min; load, 20 grams; temperature, 25° C; environment, argon; pressure, atmospheric.



(a) Body-centered cubic metals.

(b) Face-centered cubic metals.



(c) Hexagonal close-packed metals.

Figure 10. - Shear strength as a function of hydrostatic pressure for various metals. (From ref. 10.)

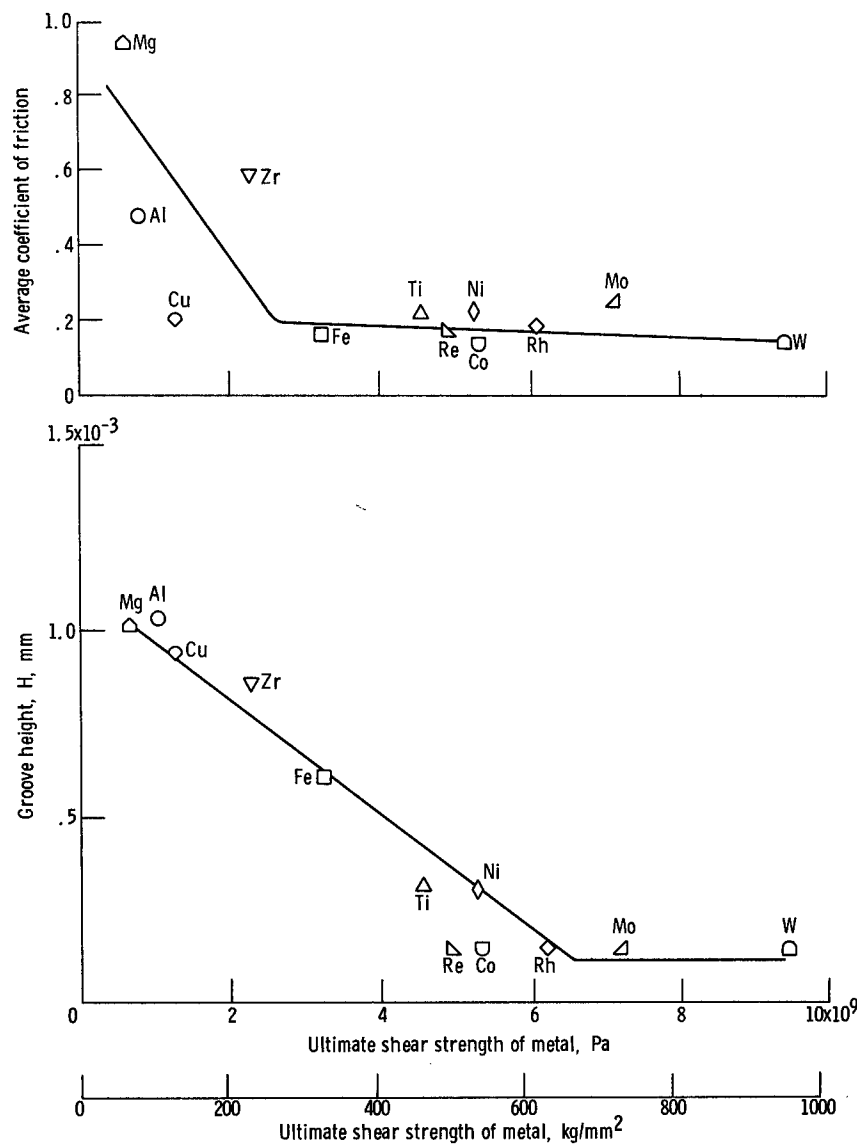


Figure 11. - Coefficient of friction and groove height as a function of shear strength for various metals. Single-pass sliding of 0.04-millimeter-radius silicon carbide rider; sliding velocity, 3 mm/min; load, 20 grams (0.2 N); temperature, 25° C; environment, argon; pressure, atmospheric.



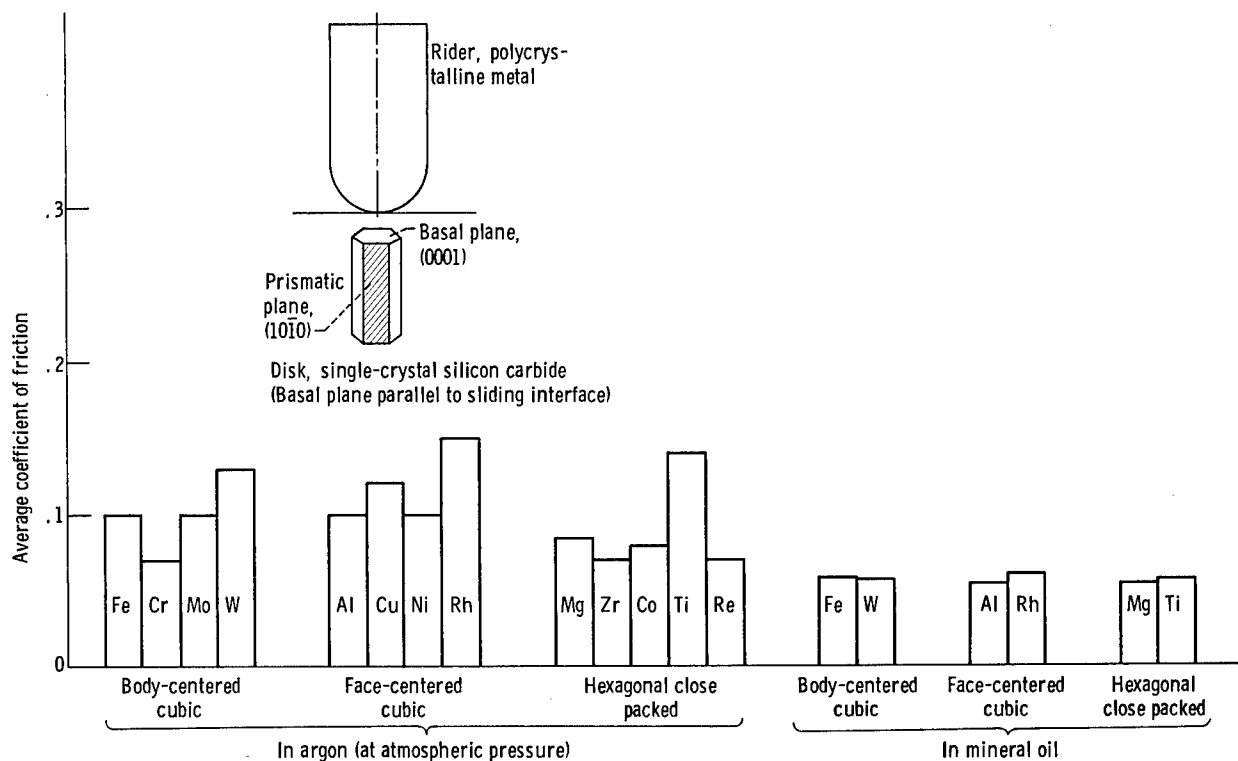


Figure 12. - Coefficient of friction for various metals sliding on single-crystal silicon carbide (0001) surface in both argon at atmospheric pressure and in mineral oil. Sliding direction,  $\langle 10\bar{1}0 \rangle$ ; sliding velocity, 3 mm/min; load, 30 grams (0.29 N); temperature, 25<sup>o</sup> C.

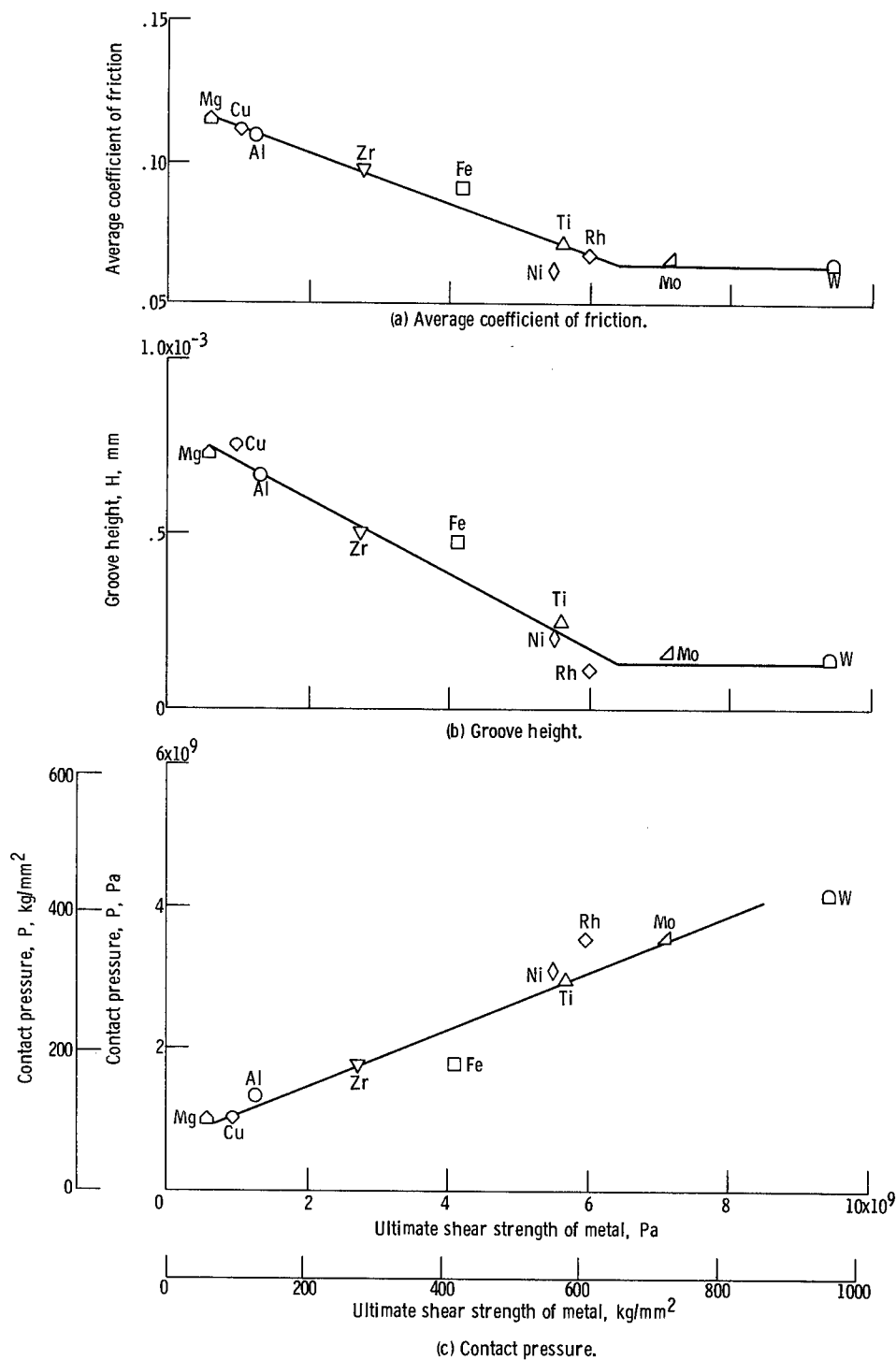


Figure 13. - Coefficient of friction, groove height, and contact pressure as a function of shear strength for various metals as a result of single-pass sliding of 0.04-millimeter-radius silicon carbide rider in mineral oil. Sliding velocity, 3 mm/min; load, 20 grams; temperature, 25° C.

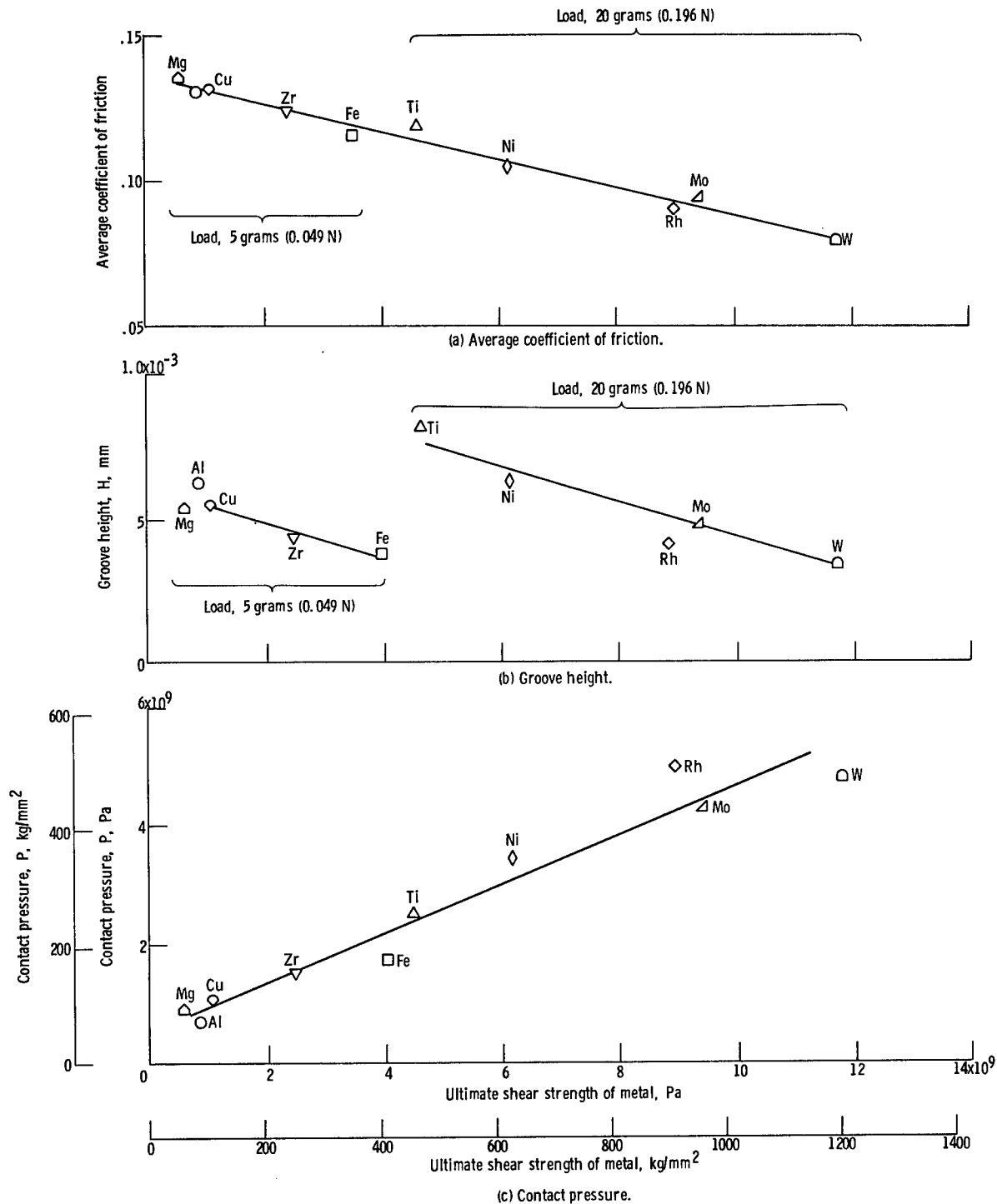


Figure 14. - Coefficient of friction, groove height, and contact pressure as a function of shear strength for various metals as a result of single-pass sliding of 0.025-millimeter-radius silicon carbide rider in mineral oil. Sliding velocity, 3 mm/min; load, 5 or 20 grams; temperature, 25° C.

|   |  |  |  |  |  |
|---|--|--|--|--|--|
| 1. Report No.<br>NASA TP-1293   |  | 2. Government Accession No.                          |  | 3. Recipient's Catalog No.   |  |
| 4. Title and Subtitle<br><b>FRICION AND WEAR OF METALS WITH A SINGLE-CRYSTAL<br/>ABRASIVE GRIT OF SILICON CARBIDE - EFFECT OF<br/>SHEAR STRENGTH OF METAL</b>   |  |  |  | 5. Report Date<br>August 1978  |  |
|   |  |  |  | 6. Performing Organization Code  |  |
| 7. Author(s)<br>Kazuhisa Miyoshi and Donald H. Buckley  |  |  |  | 8. Performing Organization Report No.<br>E-9499                            |  |
| 9. Performing Organization Name and Address<br>National Aeronautics and Space Administration<br>Lewis Research Center<br>Cleveland, Ohio 44135  |  |  |  | 10. Work Unit No.<br>506-16  |  |
|   |  |  |  | 11. Contract or Grant No.  |  |
| 12. Sponsoring Agency Name and Address<br>National Aeronautics and Space Administration<br>Washington, D.C. 20546   |  |  |  | 13. Type of Report and Period Covered<br>Technical Paper                   |  |
|   |  |  |  | 14. Sponsoring Agency Code   |  |
| 15. Supplementary Notes   |  |  |  |  |  |
| 16. Abstract<br><p>Sliding friction experiments were conducted with spherical, single-crystal silicon carbide riders in contact with various metals and with metal riders in contact with silicon carbide flats. Results indicate that (1) the friction force in the plowing of metal and (2) the groove height (corresponding to the volume of the groove) are related to the shear strength of the metal. That is, they decrease linearly as the shear strength of the bulk metal increases. Grooves are formed in metals primarily from plastic deformation, with occasional metal removal. The relation between the groove width <math>D</math> and the load <math>W</math> can be expressed by <math>W = kD^n</math>, which satisfies Meyer's law.</p> |  |  |  |  |  |
| 17. Key Words (Suggested by Author(s))<br>Abrasive wear                      Silicon carbide<br>Friction<br>Shear strength<br>Metal   |  |  |  | 18. Distribution Statement<br>Unclassified - unlimited<br>STAR Category 27 |  |
| 19. Security Classif. (of this report)<br>Unclassified  |  | 20. Security Classif. (of this page)<br>Unclassified |  | 21. No. of Pages<br>25   |  |
|   |  |  |  | 22. Price*<br>A02  |  |